

GEMATON: LIVING AND DYING IN A KUSHITE TOWN ON THE NILE

Volume IV



ARCHAEOPRESS PUBLISHING LTD

Summertown Pavilion

18-24 Middle Way

Oxford OX2 7LG

www.archaeopress.com

Sudan Archaeological Research Society

Publication Number 30

Editor of this volume: D. A. Welsby

ISBN 978-1-80327-887-2

ISBN 978-1-80327-888-9 (e-Pdf)

© The Sudan Archaeological Research Society and Archaeopress 2024

Front cover: Kawa, skeletons in grave (HA2)94.

Back cover: Skeletons in the cemetery and a bucranium in Building F1.



This work is licensed under the Creative Commons Attribution-NonCommercial-NoDerivatives 4.0 International License. To view a copy of this license, visit <http://creativecommons.org/licenses/by-nc-nd/4.0/> or send a letter to Creative Commons, PO Box 1866, Mountain View, CA 94042, USA.

This book is obtainable from The Sudan Archaeological Research Society
c/o Department of Egypt and Sudan, The British Museum, London WC1B 3DG
or from the Society's website <http://www.sudarchrs.org.uk>

Also available direct from Archaeopress or from our website www.archaeopress.com

SUDAN ARCHAEOLOGICAL RESEARCH SOCIETY
PUBLICATION NUMBER 30

**GEMATON: LIVING AND DYING IN A KUSHITE
TOWN ON THE NILE**

Volume IV

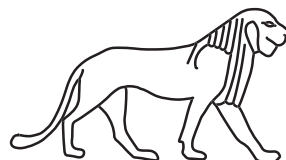
Bioarchaeology

by

Anna M. Davies-Barrett
Tatiana Vlemincq-Mendieta
Pernille Bangsgaard

with contributions by

Rebecca J. Whiting
Derek A. Welsby



**SARS
LONDON
2024**

GEMATON: LIVING AND DYING IN A KUSHITE TOWN ON THE NILE

Volume IV

Bioarchaeology

Contents

1. Introduction	1-2
<i>Derek A. Welsby</i>	
2. The Human Remains from Kawa	3-163
<i>Anna M. Davies-Barrett and Tatiana Vlemincq-Mendieta</i>	
<i>with contributions by Rebecca J. Whiting</i>	
1. Introduction	3
2. Preservation	3
3. Demography	5
3.1 Age-at-death estimation	5
Nonadult age estimation	5
Adult age estimation	5
3.2 Nonadult age distribution	5
3.3 Adult age distribution	5
3.4 Adult skeletal sex estimation	6
4. Biological variation	7
4.1 Non-metric traits	7
Adults	7
Nonadults	8
4.2 Metric data	8
Adult metric data	8
Stature	8
5. Skeletal pathology	10
5.1 Joint pathology	10
Osteoarthritis	10
Osteochondritis dissecans	11
5.2 Vertebral pathology	12
5.3 Trauma	16
Adults	16
Skull	16
Hands, feet, and patellae	16
Long bones	16
Post-cranial axial skeletal trauma	17
Instances of multiple traumatic injuries	17
Perimortem trauma	18
Nonadults	19
5.4 Periosteal reaction	20
Long bones	20
Adults	20
Nonadults	21
Sinuses	21
Ribs	21
5.5 Cranial lesions	21
Adults	21
Endocranial and ectocranial lesions	21
Enlarged arachnoid foveae	22
Nonadults	23
Endocranial and ectocranial lesions	23
Cribra orbitalia	23
5.6 Congenital and developmental abnormalities	24
Vertebrae	24
Hydrocephalus	25
Other	26

5.7 Possible neoplastic disease	27
Skeleton (561)25	27
Skeleton (HA2)209 and Skeleton (JG3)13	28
6. Oro-dental pathology	29
6.1 Tooth presence	29
6.2 Antemortem tooth loss in adults	30
6.3 Dental wear	30
6.4 Dental caries	30
Carious lesions in adults	32
Carious lesions in nonadults	32
6.5 Dental calculus	32
6.6 Periodontal disease	33
6.7 Periapical lesions	34
7. The skeleton from Building F1 Room VI	35
8. The disarticulated bone	35
9. Discussion	36
10. Kawa skeleton catalogue	40
Individual graves	40
Grid square GD3	42
Area HA1	53
Grid square HA2	59
Grid square JE2	73
Grid square JE3	74
Grid square JF2	78
Grid square JG1	80
Grid square JG2	80
Grid square JG3	86
Grid square JH3	87
Grid square JH4	93
Grid square JI4	97
Grid square FP6 in the town	98

3. The Faunal Remains from Kawa 164-199

Pernille Bangsgaard

Introduction	164
The results	164
Cattle	164
Horse/Donkey and Dromedary/Camel	166
Caprines	166
Gazelle and Antelope	167
Carnivores	167
Rodents	168
Other fauna	168
Fauna according to area of excavation	168
Site R18	170
Comparative faunal remains	170
Concluding remarks	172

4. Bibliography for Volume IV 200-206

List of Tables

2. The Human Remains from Kawa

2.1. The average percentage of completeness for each skeletal element group and for the overall completeness of each individual.	99
2.2. The proportion of individuals allocated each taphonomic score and the average score across the entire assemblage.	99
2.3. The proportion of individuals allocated each cortical surface preservation score and the average score across the entire assemblage.	99
2.4. The proportion of individuals in each nonadult age category.	99
2.5. The proportion of individuals in each adult age category.	99
2.6. The proportion of adults in each skeletal sex category, according to age group.	100
2.7. Morphological descriptions of non-metric traits and their scores.	101-104
2.8. The prevalence of cranial and mandibular non-metric traits. Prevalence according to score are provided for those traits with scoring systems other than presence/absence, as indicated by numerical scores in bold. Morphological descriptions for each numerical score are presented in Table 2.7.	105-107
2.9. The prevalence of accessory cranial sutural bones.	107
2.10. The prevalence of post-cranial non-metric traits. Prevalence according to score is provided for those traits with scoring systems other than presence/absence, as indicated by numerical scores in bold. Morphological descriptions for each numerical score are presented in Table 2.7.	108-109
2.11. Metric measurements (mm) for adult individuals, after Buikstra and Ubelaker (1994, 69-84).	110-118
2.12. Metric measurements (mm) for nonadult individuals, after Buikstra and Ubelaker (1994, 45-46).	119-123
2.13. The range and mean values for cranial and mandibular measurements (mm) in females and males. Values in brackets indicate the number of skeletal elements measured.	124-125
2.14. The range and mean values for postcranial measurements (mm) in females and males. Values in brackets indicate the number of skeletal elements measured.	126-128
2.15. Stature regression formulae (in cm) used to estimate stature in adults from Kawa (produced using ancient Egyptian populations by Raxter <i>et al.</i> 2008). m_m = Maximum length.	128
2.16. Stature estimates (cm) for individuals with femoral, tibial, humeral, or radial measurements (m_m = maximum length). The bone measurements used to calculate stature for each individual are highlighted in bold, preferentially using the bone measurement related to the equation with the smallest standard error.	128
2.17. The prevalence of osteoarthritis on different joint surfaces according to male and female sex groups, young and middle adult age groups, and in all adults (calculated for all observable joint surfaces with a completeness of 25% or more).	130-131
2.18. The prevalence of vertebral pathology in all adults, consisting of prevalence rates for osteoarthritis, osteophytes, vertebral fusion, intervertebral disc disease, Schmorl's nodes and ossification of the ligamentum flavum.	132-133
2.19. A comparison of the prevalence of vertebral pathology in young and middle adults, consisting of prevalence rates for osteoarthritis, osteophytes, vertebral fusion, intervertebral disc disease, Schmorl's nodes and ossification of the ligamentum flavum.	134-135
2.20. A comparison of the prevalence of vertebral pathology in male and female sex groups, consisting of prevalence rates for osteoarthritis, osteophytes, vertebral fusion, intervertebral disc disease, Schmorl's nodes and ossification of the ligamentum flavum.	136-137
2.21. The prevalence of skull fractures with remodelling in adults (calculated for all bones with a completeness of over 25%).	138
2.22. The prevalence of patellae, hand and foot fractures with remodelling in adults (calculated for all bones with a completeness of over 25%).	139
2.23. The prevalence of long bone fractures with remodelling in adults (calculated for all bone sections with a completeness of over 25%).	140
2.24. The prevalence of post-cranial axial skeletal fractures with remodelling in adults (calculated for all bones with a completeness of over 25%).	140
2.25. The prevalence of periosteal reaction on long bones in adults (calculated for all bone sections with a completeness of over 25%).	140
2.26. The prevalence of periosteal reaction on long bones in nonadults (calculated for all bone sections with a completeness of over 25%).	141
2.27. The prevalence of endocranial and ectocranial lesions in adults (calculated for all bones with a completeness of over 25%).	141
2.28. The prevalence of endocranial and ectocranial lesions in nonadults (calculated for all bones with a completeness of over 25%).	141
2.29. The proportion of teeth in different tooth presence categories in nonadults, according to age group and tooth type (deciduous or permanent).	142

2.30. The prevalence of antemortem tooth loss by tooth site in adults.	143
2.31. Average wear scores for each of the anterior teeth according to male and female sex groups, young and middle adult age groups, and in all adults. The number of teeth observed for wear in each tooth class is presented in brackets.	144
2.32. Average wear scores for each of the molars according to male and female sex groups, young and middle adult age groups and in all adults. The number of teeth observed for wear in each tooth class is presented in brackets	145
2.33. The prevalence of carious lesions by tooth according to male and female sex groups, young and middle adult age groups and in all adults.	146-147
2.34. The prevalence of carious lesions by deciduous tooth in infancy, early childhood and late childhood age groups, and in all nonadults.	148
2.35. The prevalence of carious lesions by permanent tooth in late childhood, puberty and adolescence age groups and in all nonadults.	149-150
2.36. The percentage of individuals with at least one observable tooth with calculus present, according to permanent or deciduous dentition and age group.	150
2.37. The prevalence of periodontal disease scores in all adults according to position of the alveolar crest.	151
2.38. The prevalence of periodontal disease scores in male and female sex groups according to position of the alveolar crest.	152-153
2.39. The prevalence of periodontal disease scores in young adult and middle adult age groups according to position of the alveolar crest.	154-155
2.40. The prevalence of periapical lesions in adults according to male and female sex groups, young and middle adult age groups and in all adults. 1 = smooth-walled cavity; 2 = rough-walled cavity.	156-157
2.41. Descriptions of disarticulated remains recovered from Kawa.	158-163

3. The Faunal Remains from Kawa

3.1. Distribution of mammalian species identified in the Kawa collection.	172
3.2. Distribution of other species identified in the Kawa collection.	173
3.3. Distribution of cut- and chop-marks in the Kawa collection according to bone and location.	175-177
3.4. Distribution of state-of-fusion for cattle long-bones from Kawa.	177
3.5. All measurements taken on cattle remains in the Kawa collection.	178-194
3.6. Direct comparison of measurements of the metapodiums and calcaneus between the sites of Kawa and Kerma. The latter measurements are published by Louis Chaix (Chaix 2007).	194
3.7. All measurements taken from other species in the Kawa collection.	195
3.8. Distribution of state-of-fusion for goat (NISP 55) long bones from Kawa.	196
3.9. Distribution of state of fusion for sheep/goat (NISP 58) long bones from Kawa.	196
3.10. All measurements taken on goat remains in the Kawa collection.	197
3.11. Distribution of species at Kawa according to excavation area.	198
3.12. Distribution of species comparing faunal result from various sites.	199

List of Figures

1. Introduction

1.1. Sites in Sudan mentioned within the reports. 2

2. The Human Remains from Kawa

2.1. The frequency of individuals in each age category. 6

2.2. The frequency of adults in each combined skeletal sex category, according to age group. 7

2.3. A box and whisker plot comparing femoral head diameter (mm) in female and male sex groups. The boxes represent the 25th and 75th quartiles and the whiskers represent the full range of measurements. Individuals of undetermined sex with femoral head measurements are marked on the chart separately. Those in blue represent individuals whose measurement falls below the female 75th quartile, those in green represent individuals whose measurement falls above the male 25th quartile, and those in red represent individuals whose measurement falls within the overlapping range of both male and female measurements. 9

2.4. A box and whisker plot comparing humeral head diameter (mm) in female and male sex groups. The boxes represent the 25th and 75th quartiles and the whiskers represent the full range of measurements. Individuals of undetermined sex with humeral head measurements are marked on the chart separately. Those in blue represent individuals whose measurement falls below the female 75th quartile, those in green represent individuals whose measurement falls above the male 25th quartile, and those in red represent individuals whose measurement falls within the overlapping range of both male and female measurements. 9

2.5. A box and whisker plot comparing stature estimates (cm) in female and male sex groups. The boxes represent the 25th and 75th quartiles and the whiskers represent the full range of stature measurements. 10

2.6. The skeletal distribution of osteoarthritis on non-vertebral joints in all adults (prevalence displayed in 10% increments). Image adapted from Buikstra and Ubelaker (1994). 11

2.7. The prevalence of vertebral pathology in all adults according to vertebra, consisting of prevalence rates for osteoarthritis, osteophytes, intervertebral disc disease, Schmorl's nodes and ossification of the ligamentum flavum. 13

2.8. The skeletal distribution of periosteal reaction on the long bones in all adults (prevalence displayed in 5% increments). Image adapted from Buikstra and Ubelaker (1994). 20

2.9. The prevalence of antemortem tooth loss by tooth site in all adults. 30

2.10. Mean wear score values for the anterior dentition (blue dots) in all adults and standard error bars. 31

2.11. Mean wear score values for the molars (blue dots) in all adults and standard error bars. 31

2.12. The prevalence of carious lesions by tooth in all adults. 32

2.13. The prevalence of carious lesions by tooth in female and male sex groups. 32

2.14. The prevalence of carious lesions by tooth in nonadults according to deciduous and permanent dentition. 33

2.15. The prevalence of periodontal disease scores 2 to 5 in all adults according to alveolar crest. 34

2.16. The prevalence of scores 1 (smooth-walled cavity) and 2 (rough-walled cavity) for periapical lesions in adults according to tooth site. 35

3. The Faunal Remains from Kawa

3.1. Distribution of body parts for cattle and large ungulate remains from Kawa. 165

3.2. Kill-off profile for cattle based on tooth eruption and wear (NISP 84). 166

3.3. Distribution of species at Kawa according to excavation area. The carnivore group includes all dog and cat remains, the other group includes rodent, frog/toad and crocodile remains. 169

3.4. Distribution of species from comparative sites. 171

List of Plates

2. The Human Remains from Kawa

2.1. Taphonomic changes to the cortical surfaces of bone.	4
A. Dark mottled staining on a fragment of right parietal [Skeleton (JE3)187].	
B. Termite damage to the patellofemoral joint surface of the left femur, mimicking bone destruction caused by pathological changes [Skeleton (GD3)127].	
2.2. A suprattrochlear spur (arrow) present on the right humerus of a nonadult [Skeleton (GD3)114].	8
2.3. Impingement syndrome of the left shoulder joint in a middle adult probable female [Skeleton (561)21].	11
A. Eburnation and osteophyte formation on the inferior aspect of the acromion process.	
B. Corresponding changes to the humeral head, including eburnation, pitting and new bone formation on the joint surface.	
2.4. Osteochondritis dissecans of the medial condyle of the left femur, with associated 'joint mouse', in an adolescent [Skeleton (HA2)247].	12
Top: Joint mouse and associated divot within the medial condyle shown separately.	
Bottom: Joint mouse shown within divot as it would have been located anatomically in life.	
2.5. Rounded perforations on the sixth cervical vertebra in a middle adult probable female, located on the inferior surface and posterior-inferior margin of the vertebral body [Skeleton (HA2)164].	13
2.6. Destruction of the twelfth thoracic vertebra in a young adult male, located on the superior aspect of the vertebral body and accompanied by porosity and remodelling [Skeleton (HA2)124].	14
2.7. Destruction and porosity on the superior-anterior margin of the first sacral vertebra in a middle adult of unknown sex [Skeleton (JH3)125].	14
2.8. Destruction and porosity on the superior-anterior margin of the fourth lumbar vertebra in a young adult of unknown sex [Skeleton (JH4)108].	14
2.9. A compression fracture of the sixth thoracic vertebra in a young adult male, causing a height difference in the lateral aspects of the vertebral body and likely producing a slight scoliotic curve [Skeleton (HA2)209].	14
2.10. Diffuse idiopathic skeletal hyperostosis (DISH) in an adult male of unknown age. Prolific osteophyte formation on the right anterior-lateral aspects of the thoracic and upper lumbar vertebral bodies, causing spinal fusion [Skeleton (HA2)259].	15
2.11. Large cavitations/hypervascularity on the anterior aspect of a thoracic vertebral body in an adolescent [Skeleton (1055)6].	15
2.12. The vertebrae of an adolescent affected by Scheuermann's disease [Skeleton (HA2)247].	15
A. A large Schmorl's node on the inferior aspect of the sixth thoracic vertebral body.	
B. Fine, diffuse porosity on the anterior aspect of a thoracic vertebral body.	
2.13. A depression on the left aspect of the cranium (arrow) in the region of the coronal suture in a middle adult probable female [Skeleton (HA2)168].	16
2.14. Misaligned healed fractures of the left tibia and fibula in a middle adult male [Skeleton (HA2)169].	17
2.15. Possible perimortem sharp-force trauma in a young adult female [Skeleton (JG3)13].	18
A. The lateral aspect of the left iliac blade, demonstrating a circular perforation and slight bevelling.	
B. The ectocranial surface of the right parietal, demonstrating a 'keyhole' fracture (arrow).	
2.16. The disorganised nature of Skeleton (JG3)13 within the grave when excavated, likely due to looting.	18
2.17. The position of Skeleton (HA2)209 within the grave when excavated. Note the prone position of the skeleton and disarticulated nature of the vertebrae.	19
2.18. Potential sharp-force trauma in a young adult male on the left superior articular facet of the fourth lumbar vertebra (arrow) [Skeleton (HA2)209].	19
2.19. Possible blunt force trauma in a middle adult female with plastic deformation to the posterior aspect of the cranium [Skeleton (HA2)198].	19
2.20. A possible childhood fracture affecting the distal third of the right ulna of an adolescent [Skeleton (1055)6].	19
A. Lateral curvature of the distal third of the right ulna (red arrow); not apparent on the left ulna.	
B. Radiograph of the right ulna with a very faint radiopaque line at the apex of the lateral curvature (white arrow and box), possibly indicating a healed childhood fracture.	
Radiograph by Dr Daniel O'Flynn.	
2.21. Examples of periosteal reaction on the tibiae.	20
A. New woven bone on the proximal portion of the right tibial shaft in a middle adult probable male [Skeleton (HA2)255].	
B. Remodelled porous lamellar bone on the distal portion of the left tibial shaft, causing thickening	

of the shaft, in a young adult of unknown sex [Skeleton (JH4)108].	
2.22. Nodular new bone formation in a probable male of unknown age on the endocranial surface of the frontal in the region of the frontal crest, possibly representing hyperostosis frontalis interna [Skeleton (JG2)43].	22
2.23. Enlarged arachnoid foveae on the endocranial surfaces in a middle adult probable male [Skeleton (HA2)255].	22
A. Multiple coalesced lesions on the endocranial surface of the left greater wing of the sphenoid, including a large deep cavity with remodelled rounded margins and floor.	
B. Multiple, sometimes coalesced, lesions on the endocranial surface of the left parietal along the sagittal sulcus. Some lesions were remodelled, with rounded margins, while others had sharp margins and undercutting.	
2.24. New bone formation on the endocranial surface of the occipital in a young child [Skeleton (HA2)102].	23
2.25. An advanced porous orbital roof lesion in the left orbit of a young child [Skeleton (HA2)102].	23
2.26. The seventh cervical vertebra of a nonadult, demonstrating a cranial border shift with associated cervical ribs [Skeleton (GD3)86].	24
2.27. Spondylosis of a sixth lumbar vertebra in a middle adult male [Skeleton (GD3)69].	24
2.28. The first cervical vertebra of a child, demonstrating a cleft posterior neural arch [Skeleton (GD3)114].	24
2.29. A complete sacral neural arch hiatus in a nonadult [Skeleton (GD3)86].	25
2.30. Skeleton (GD3)154, an infant, located within the grave with cranium intact, demonstrating expansion of the cranium, advanced cranial bossing, and an extremely enlarged anterior fontanelle, all likely related to the condition of hydrocephalus.	25
2.31. The two frontal halves of the infant with hydrocephalus, demonstrating an extremely enlarged anterior fontanelle [Skeleton (GD3)154].	25
2.32. Agenesis or craniosynostosis of the sagittal and temporal sutures in a middle adult male, leading to elongation of the cranial vault from anterior to posterior, known as scaphocephaly [Skeleton (JG2)312].	26
2.33. The lateral aspect of the iliac crest of the left ilium of a middle adult male, showing destruction of the iliac crest and blade (white arrows) and new bone formation. In regions of postmortem damage, new bone can be observed embedded within the trabeculae and extending beyond the destructive foci (red arrow) [Skeleton (561)25].	27
2.34. Diffuse nodular woven bone on the inferior aspect of the fifth lumbar vertebral body in a middle adult male [Skeleton (561)25].	27
2.35. The left ilium of a middle adult male with mixed destruction and new bone formation, possibly caused by pathological changes related to metastatic cancer [Skeleton (561)25].	28
A. Destruction (white arrow) and the extent of visible new bone formation within the trabeculae (red arrows) on the medial surface of the ilium.	
B. A radiograph of the left ilium, demonstrating slight sclerotic margins around lytic lesions (white arrow). Dense radiopaque regions (red arrow) are likely caused by the infiltration of earth into the trabeculae postmortem. Radiograph by Dr Daniel O'Flynn.	
2.36. New bone formed within the mandibular canal on the left side of the mandible in a young adult female [Skeleton (JG3)13].	29
A. The granular, slightly-porous new bone is located within the mandibular canal, but is not integrated with the surrounding cortical bone.	
B. Image segmentation using a CT scan of the affected mandible illustrates the possible dimensions of the tumour-like new bone (orange region). CT scan and image manipulation by Dr Daniel O'Flynn.	
2.37. A large periapical lesion (arrow) in an adult, located within the left maxillary alveolar bone in the region of the first premolar [Skeleton (HA2)171].	34
2.38. Skeleton (FP6)30 <i>in situ</i> within Room VI of Building F1.	35
2.39. Skeleton (GD3)154, an infant, within the grave, demonstrating its careful burial and the inclusion of blue bead bracelets and anklets on the body when buried.	38

3. The Faunal Remains from Kawa

3.1. Three examples of fractured 1 st phalanges from Kawa.	165
3.2. Animal bones in Building A2, Room II (photo: D. A. Welsby).	170
3.3. Animal bones within deposits seen in section in the doorway between Rooms VI and VII in Building A2 (photo: D. A. Welsby).	170
3.4. Cattle horn core resting on the sloping surface of the descender in grave (JG1)12 (photos: D. A. Welsby).	171
3.5. Sheep and goats grazing in the Seleim Basin with one of the seasonal lakes in the background (photo: D. A. Welsby).	173

1. Introduction

Derek A. Welsby

It had been the intention to devote this volume to reports on the bioarchaeological material recovered during the excavations at Kawa between 1997 and 2018. Unfortunately the report on the floral remains is delayed and therefore, so as not to hold up the publication of the human and animal bone, is not included here. For a report on some of the archaeobotanical material from Kawa, published in *Sudan & Nubia*, see Fuller 2004.

The designation of graves and skeletons in the report on the human remains is in the format (grid square)context number in most cases. However a small number of graves in the cemetery, site R18, was visible on the surface and each of these was excavated individually. In those cases the number in curved brackets is the feature number relating to the survey of the site in 1993 and following the location of grave cuts on the surface during the 2000 season. All feature numbers between (1055) and (1083) were subsequently grouped into Area (HA1).

The articulated human skeletons were excavated either by the physical anthropologist present as a member of the Sudan Archaeological Research Society's team or by some of the particularly skilled local workmen under the general supervision of the anthropologist. Bodies were recorded *in situ* and lifted and bagged by the physical anthropologist, two of whom are among the authors of the report published here.

Physical anthropologists present in the field:-

2000	January-March	Margaret Judd
2000-1	December-February	Margaret Judd
2001-2	December-February	Margaret Judd
2007-8	December-February	Iwona Kozieradzka
2009-10	December-February	Emilie Gustafsson
2010-11	December-February	Natasha Kalogirou
2013	January-February	Rebecca Whiting
2013-14	December-February	Rebecca Whiting
2014-15	December-February	Bonnie Knapp
2017	January-March	Tatiana Vlemincq-Mendieta
2017-18	December-February	Tatiana Vlemincq-Mendieta

During, and on the completion of, the excavation project the skeletal material was donated to SARS by the National Corporation for Antiquities and Museums and, with its permission, passed on to the British Museum for permanent curation. Once there it was studied in detail in the Barbara Mertz Bioarchaeology Laboratory within the Department of Egypt and Sudan. The EA Number noted in the catalogue of the human bone is the object number of each skeleton accessed into the collections of the Department of Egypt and Sudan.

The animal remains were recovered during the excavation of the deposits in which they lay. Unfortunately it did not

prove possible for the archaeozoologist to examine them *in situ* and their fragility in many cases resulted in considerable fragmentation of the material. An initial study of some of the material was made by Kim Burrows based in the excavation house in the 2009-10 season and by Pernille Bangsgaard in the 2008-9 and 2010-11 seasons.

In Volume I of the Kawa reports the presence of human and animal bones is recorded based on the information available immediately before the report went to press. Subsequently, during the completion of the Bioarchaeology volume, a small amount of additional material was examined. Where this material is not mentioned in Volume I attention is drawn to this fact so that this material can be taken into account when reading, in particular, the report on the excavation in the cemetery.

The sites in Sudan mentioned within the reports are located on Figure 1.1.

Dr Patricia Spencer kindly copy edited this volume. Any remaining errors are the full responsibility of the individual authors.



Figure 1.1. Sites in Sudan mentioned within the reports.